Published in final edited form as:
Land Degrad Dev. 2018 June ; 29(6): 1896–1905. doi:10.1002/ldr.2976.

Measuring ephemeral gully erosion rates and topographical thresholds in an urban watershed using unmanned aerial systems and structure from motion photogrammetric techniques

Napoleon Gudino-Elizondo[a], **Trent Biggs**[b], **Carlos Castillo**[c], **Ronald Bingner**[d], **Eddy Langendoen**[d], **Kristine Taniguchi**[b], **Thomas Kretzschmar**[a], **Yongping Yuan**[e], and **Douglas Liden**[f]

[a.]Centro de Investigación Científica y de Educación Superior de Ensenada (CICESE), Carretera Ensenada-Tijuana 3918, Zona Playitas, 22860 Ensenada, B.C., México

[b.]Department of Geography, San Diego State University, 5500 Campanile Dr., San Diego, CA 92182-4493

[c.]Department of Rural Engineering, University of Córdoba, Córdoba, Spain

[d.]National Sedimentation Laboratory, Agricultural Research Service, USDA, Oxford, MS, 38655

[e.]USEPA Office of Research and Development, Research Triangle Park, NC 27711

[f.]USEPA San Diego Border Liaison Office, 610 West Ash St., Suite 905, San Diego, CA 92101

Abstract

Both rural and urban development can lead to accelerated gully erosion. Quantifying gully erosion is challenging in environments where gullies are rapidly repaired, and in urban areas where microtopographic complexity complicates the delineation of contributing areas. This study used unmanned aerial vehicles (UAVs) and Structure-from-Motion (SfM) photogrammetric techniques to quantify gully erosion in the Los Laureles Canyon watershed, a rapidly urbanizing watershed in Tijuana, Mexico. Following a storm event, the gully network extent was mapped using an orthomosaic (0.038 m pixel size); the local slope and watershed area contributing to each gully head were mapped with a Digital Surface Model (0.3 m pixel size). Gullies formed almost exclusively on unpaved roads which had erodible soils and concentrated flow. Management practices (e.g. road maintenance that fill gullies after large storms) contributed to total sediment production at the watershed scale. Sediment production from gully erosion was higher and threshold values of slope and drainage area for gully incision were lower than ephemeral gullies reported for agricultural settings. This indicates high vulnerability of unpaved roads to gully erosion which is consistent with high soil erodibility and low critical shear stress measured in the laboratory with a mini jet-erosion-test device. Future studies that evaluate effects of different soil types on gully erosion rates for unpaved roads, as well as those that model effects of management practices such as road paving and their impact on runoff, soil erosion, and sediment loads are needed to advance sediment management and planning in urban watersheds.

Conflict of Interest
The authors declare no conflict of interest.

Keywords

Gully erosion; Topographic thresholds; Structure-from-Motion; Unmanned Aerial Vehicles (UAV); Urbanization; Watershed management

Introduction

In New Zealand, serious problems exist in the North Island's East Coast region, where the widespread deforestation of soft-rock hill country by European settlers over the last century (Allsop, 1973) has led to severe hillslope erosion and soil loss, and consequent flooding and sedimentation downstream (Trustrum et al., 1999; Page et al., 2001).

Gully erosion is often associated with land degradation caused by anthropogenic activities and is commonly related to changes in catchment hydrology, such as removal of native vegetation and soil disturbance (Oygarden, 2003). Gully characteristics and erosion rates have been well documented in agricultural environments, but high erosion rates are also observed in urban areas during construction (Wolman, 1967). Erosion rates usually decline as the urban landscape matures (Archibold, Levesque, de Boer, Aitken, & Delanoy, 2003), but this is not always the case in developing countries where soil exposure can last for decades following urbanization (Biggs, Atkinson, Powell, & Ojeda, 2010). This can result in chronically high gully erosion rates compared with undisturbed areas or urban areas with high impervious and/or vegetation cover.

There are few studies assessing gully erosion in urban settings (Castillo & Gómez, 2016). Adediji, Jeje, and Ibitoye (2013) described the relationship between urban land surface characteristics and gully erosion in Nigeria and found a significant relationship between soil texture and land use. Other studies describe the expansion and headcut retreat of permanent urban gullies. Archibold et al. (2003) surveyed two urban gullies from 1994 to 2000 and measured gully headcut retreat, widening, and deepening. They attributed gully erosion to land-use change, as was also found by Guerra and Hoffman (2006) in Brazil and by Imwangana, Dewitte, Ntombi, and Moeyersons (2014) in Congo. Nevertheless, little has been done to characterize erosion rates for a large network of gullies, due in part to difficulty in surveying them.

Ephemeral gullies can be important contributors to sediment production at the watershed scale (Vandaele, Poesen, Govers, & van Wesemael, 1996), especially in arid and semiarid environments. Such gullies are small eroded channels formed by concentrated runoff during a storm event (Foster, 1986) and are temporary features removed by tillage operations (Poesen & Govers, 1990) or filled with sediment in urban environments. Ephemeral gullies form from a complex interaction between physical and management attributes such as topography, rainfall duration and intensity, soil moisture, soil properties, vegetation cover, and management practices (Momm, Bingner, Wells, & Wilcox, 2012). An ephemeral gully will form only when a particular interaction between these attributes, or an abrupt change in ground surface elevation, leads to shear stress caused by overland runoff exceeding the soil critical shear stress to produce scour below the soil surface and eventually incision or upstream migration of the gully head (GH). A *GH* is the location at which gully erosion

processes cannot continue upstream under particular combination of rainstorm intensity, storm discharge, land use, vegetation cover, and soil type (Torri & Poesen, 2014).

Several studies have documented the relationship between ephemeral gully formation and runoff erosivity using topographic attributes, especially drainage area (Ad) and local slope (S) at the GH, with a threshold defined by $S = aA_d^b$ (Foster, 1986; Montgomery & Dietrich, 1994; Patton & Schumm, 1975; Thorne, Zevenbergen, Grissinger, & Murphey, 1986). In this equation, 'a' is a constant that varies with lithology, soils, climate, and vegetation cover (Vandaele et al., 1996), and "b" is an exponent related to the dominant processes that form the gully (Gómez-Gutiérrez, Schnabel, & Lavado-Contador, 2009). Montgomery and Dietrich (1994) suggested that b = 0.5 for laminar flow and b = 0.86 for turbulent flow. *S* has been measured using different methods such as clinometer, compass, topographic maps, and digital elevation models (DEMs). Recently, three-dimensional photo-reconstruction techniques have been used to estimate slopes in soil erosion studies (Castillo, James, Redel-Macías, Pérez, & Gómez, 2015; Di Stefano, Ferro, Palmeri, & Pampalone, 2017; Gómez-Gutiérrez, Schnabel, Berenguer-Sempere, Lavado-Contador, & Rubio-Delgado, 2014; Nadal-Romero, Revuelto, Errea, & López-Moreno, 2015) but have not been applied in characterizing ephemeral gullies in an urban context.

Ephemeral gullies can be identified and characterized using aerial imagery because they commonly have distinct color, texture, and shadow characteristics (Gómez-Gutiérrez et al., 2009) that differ from the rest of the landscape. Aerial imagery complements ground surveys of gully erosion, especially for rapidly urbanizing watersheds in developing countries, where ground surveys are difficult due to formation of large gullies on unpaved roads, stream channel bank collapse, landslides, and flooding that impede field access. Urban gullies are often filled in within days of formation and require rapid assessment after a storm. Remote sensing supported by ground control points (GCPs) is often quicker and covers a larger area than manual surveys. GCPs are critical to scale and georeference the remote sensing-derived cartographic products.

Many studies use time series of aerial photographs to map gully erosion, mostly in natural and agricultural areas (Nachtergaele & Poesen, 1999; Parkner, Page, Marutami, & Trustrum, 2006; Ries & Marzolff, 2003). *DEMs* derived from aerial imagery have also been used (Martínez-Casasnovas, Ramos, & Ribes-Dasi, 2002; Thorne et al., 1986). More recently, structure from motion (SfM) has been used in geomorphic studies, including different spatial scales, environments, and applications (Di Stefano et al., 2017; Gómez-Gutiérrez et al., 2014; James & Robson, 2012; Micheletti, Chandler, & Lane, 2014; Turner, Lucieer, & Watson, 2012; Westoby, Brasington, Glasser, Hambrey, & Reynolds, 2012). *SfM* is a photogrammetric technique based on computer visualization tools and image-based, three-dimensional surface reconstruction algorithms (James & Robson, 2012). *SfM* creates massive point clouds based on pixel matching from which highly accurate digital surface models (DSMs), *DEMs*, and orthophotos can be derived. Accuracy of *SfM* in assessing gully erosion is very similar to the most accurate topographic methods such as terrestrial laser scanning or traditional photogrammetry (Castillo et al., 2012; Fonstad, Dietrich, Courville, Jensen, & Carbonneau, 2013; James & Robson, 2012), but *SfM* is cheaper and faster (Castillo et al., 2015; Westoby et al., 2012). High spatial resolution orthophotos

derived from *SfM* can be used to identify the location of gully networks and key characteristics of gully formation such as S and A_d and their relationship with soil loss within a gully network (Gómez-Gutiérrez et al., 2014).

Gully networks, whether in agricultural or in urban areas, have characteristic patterns of sediment production pertaining to A_d. Large watersheds usually have low normalized (per unit area) sediment production compared with small watersheds, because they have more storage capacity to retain sediment and the average slope decreases with increasing watershed size (Castillo & Gómez, 2016; Walling, 1983); this has also been reported for gully erosion rates (Poesen, Nachtergaele, Verstraeten, & Valentin, 2003; Vanwalleghem, Poesen, Nachtergaele, & Verstraeten, 2005). Poesen et al. (2003) and Castillo and Gómez (2016) compiled gully erosion rates for different agricultural environments, but ephemeral gully erosion rates and topographic thresholds for gully initiation in urbanized watersheds are not available.

This paper aims to map gullies and quantify gully erosion rates using unmanned aerial systems (UASs)-based *SfM* technology to aid understanding of the processes of gully formation in Los Laureles Canyon Watershed (LLCW), a rapidly urbanizing watershed that drains into the Tijuana Estuary in the western section of the United States–Mexico border. It addresses three questions aligned with the objectives: (a) Where do gullies form in an urbanizing landscape in a developing country context? (b) What are the management implications for the control of sediment production? and (c) How do the topographic thresholds for gully formation (S and A_d) and sediment production rates from urban gullies compare with gullies in agricultural settings? The study is novel in presenting topographic thresholds for ephemeral gully formation and erosion rates in an urban environment, using a combination of *UASs–SfM* photogrammetric techniques.

Methods

Study Area

The San Bernardo (SB) neighborhood (20 ha, Figure 1) is located in the Los Laureles Canyon Watershed (LLCW), a bi-national watershed that flows from Tijuana, Mexico, into the southwestern arm of the Tijuana Estuary, United States. (Figure 1). The climate is Mediterranean, with a wet season from November to April and annual precipitation of ~24 cm/yr. Most storms occur in winter. *SB* is located on the San Diego formation, which includes deposits of erosive and loosely consolidated sandstone and siltstone, with average slope of 15 degrees. Excessive erosion, transport and deposition of sediment in the *LLCW* watershed have had many detrimental impacts on the people living in the watershed and have impaired ecosystems in the Tijuana Estuary (Weis et al., 2001).

Image acquisition and processing

Both ground- and UAV-based surveys of a gully network that formed following a large storm event on January 5-7, 2016 were conducted on January 16, 2016 (Figure 2). The storm was the largest of the water year (~50 mm), and had a 15-minute maximum intensity of 4.8 mm, which has a 1-year recurrence interval. Other storms occurred during the year, but were

smaller than the threshold precipitation typically required to produce gullies in *SB* (~25-35 mm), as observed on other field visits following storm events during three hydrological years (2013-2016). The volume of sediment generated by the gullies during the January storm was therefore used as the annual total for comparison to other studies. The 2016 water year (October 2015-September 2016) was drier than normal (155 mm total precipitation vs long-term average of 238 mm), so our results likely underestimate the long-term mean sediment production from gullies in this location.

Aerial imagery was acquired during two flights over the *SB* neighborhood. Digital true color images were acquired using a nonmetric, commercially available digital camera (GoPro, 12 megapixels resolution) mounted on a *UAV* (DJI Phantom 2). The camera was set to time-lapse capture mode (1 image per second) and images were acquired at an altitude of 75 m (above ground level) to ensure 75% side overlap and 75% forward overlap. The camera mounted facing 15 degrees from vertical to avoid doming deformations (James & Robson, 2014).

SfM was used to create a *DSM* using 7 *GCPs* (calibration points, Table S1) and 6 error control points (ECPs or validation points, Table S2) spatially distributed over the study area (Figure 3) and surveyed using differential GPS (Magellan Pro Mart 3) with sub-centimeter to 5 cm vertical accuracy (Magellan Systems Corporation, San Dimas, USA). Other researchers have documented that using 4 to 5 *GCPs* with additional *ECPs* could be considered to determine relatively small but widely distributed surface changes (James, Robson, d'Oleire-Oltmanns, & Niethammer, 2017) and that root mean square errors (RMSEs) can be reduced by placing *GCPs* on the image perimeter (Vericat et al., 2009). A dense point cloud (11 points/m^2) was generated using the Agisoft Photoscan Professional software (Agisoft LCC, Russia, Version 1.3.0) from which an orthophoto (0.038-m spatial resolution) and a *DSM* (0.3-m spatial resolution) were created. The spatial resolution (0.3 m) was calculated as √(1/d), where *d* is the SfM-derived point density, which resulted in one point, on average, in every 0.3 × 0.3 m pixel.

The error of the *DSM* georegistration was measured as the vertical and horizontal difference between validation (ECP) coordinates and corresponding *X*–*Y* or *Z* coordinate values from the *DSM*. The *RMSE* for *ECPs* was calculated as

$$RMSE = \sqrt{\frac{1}{n}\Sigma_{i=1}^{n}(dGPScoordinate\_i - DSMcoordinate\_i)^2} \quad (1)$$

where *i* is the index of the *GCP* or *ECP* points, and 'n' is the number of *GCPs* (7) or *ECPs*. Additionally, geometry of the orthophoto was tested comparing lengths of 10 different elements (sewer structures) in the image to field data (Table S3). This was deemed as the most appropriate measure of accuracy since the goal was to map dimensions of the gullies, not determine their absolute position.

Topographic thresholds

GHs were identified using the orthophoto (Figure 3), and their topographic attributes (S and A_d) were measured using *DSM* data. Flow paths and watershed boundaries for each GH, and for various locations along the gully network, were delineated using Hydrology tools in ArcGIS 10.2. A *GH* was defined as a channel at least 30 cm wide in the uppermost stream cross section. *GHs* are defined operationally for a given purpose; here, we used 30 cm based on the resolution of the imagery and the width of *GH* observed in the field. S was calculated as the slope gradient of the DSM-derived flowpath over a distance of 2 m upstream from each *GH*. A_d was the area draining into each *GH* calculated from the SfM-derived *DSM* using the Hydrology tools in ArcMap 10.2. The threshold combination of S and A_d that generates gullies was determined by fitting the equation $S = aA_d^b$ to the lower envelope of the S–A_d plot.

Our method to calculate S follows previous gully erosion studies that use *DSMs* to calculate upslope lengths (i.e., Gómez-Gutiérrez et al., 2014). Our use of 2 m for the upslope length is similar to Vandekerckhove, Poesen, Oostwould Wijdenes, and de Figueiredo (1998), who used a range from 2 to 4 m. Most studies do not use a constant upslope length, but rather use the nearest two contour lines upslope of each *GH* to define the upslope segment, and do not report an upslope length (Table S4). In order to determine the sensitivity of a and b to upslope length, both a and b were also determined using upslope distances of 2, 3, and 5 m to calculate S (see Supporting Information).

Specific Soil Loss (SSL)

Fourteen watersheds (Figure 3) were delineated using the watershed tool in ArcGIS 10.2, and were used to estimate gully erosion rates. Watershed outlets were defined by the downslope terminus of the gully network, and watershed sizes spanned the range generally observed in *SB*. Gully widths and depths were hand-measured in the field, with a ruler, at 48 locations to calibrate and validate the gully dimensions estimated by remote sensing. Polygons of gully perimeter were delineated manually by visual interpretation of the orthophoto. Gullies were too narrow and deep to estimate depth from the DSM, so a uniform depth was estimated for each polygon using visual interpretation informed by the field measurements. The volume eroded was calculated as the product of the polygon area times estimated depth. The specific soil loss (SSL, the average depth of soil loss in the watershed), was then calculated for each watershed as the total gully erosion (m^3) normalized by A_d (Figure 4).

Mini-jet test analysis

Five soil samples were collected at representative sites under different land cover conditions (natural, gully walls and filled roads) over the study area to estimate the critical shear stress and soil erodibility using a mini-jet-erosion test following Hanson (1990) and Al-Madhhachi et al. (2013).

Results

SfM-derived *DSM*

The mean absolute error between observed and modeled object lengths was 2 cm (Table S3), which is 7% of the smallest features we measured, and is the most appropriate error statistic for mapping gully dimensions. The *RMSE* for *ECPs* was 3 cm in the X–Y and 7 cm in the Z (Table S2). The SfM-derived *DSM* had relatively similar (i.e., lower) errors compared with other *SfM* applications (Dietrich, 2016; Javernick, Brasington, & Caruso, 2014; Vericat et al., 2009). This magnitude of error is acceptable for the smallest features we mapped, which were approximately 30-cm-wide gullies. The relative precision ratio (measurement precision: observation distance) was 1:833, which is similar to 1:950 reported by James and Robson (2012) to evaluate three-dimensional photo reconstruction quality in *SfM* applications.

Topographic thresholds

A total of 30 *GHs* were identified by the SfM-derived orthophoto. S correlated inversely with A_d at the *GHs* (Figure 5), which is consistent with previous studies (Castillo & Gómez, 2016; Kakembo, Xanga, & Rowntree, 2009; Montgomery & Dietrich, 1992; Torri, Sfalanga, & Chisci, 1987; Vandaele et al., 1996; Vanwalleghem et al., 2005). The line fitted through the lower envelope of the S–A_d relationship depicts threshold values required for gully formation (Patton & Schumm, 1975). For instance, an S value of 0.015 and/or an A_d of 0.0008 ha (8 m^2) are needed to initiate gully erosion under the rainfall and erodibility conditions in the study area (Figure 5).

The mean topographic attributes equation ($S = 0.02^* A_d^{-0.36}$) was similar to the one reported by Vandaele et al. (1996) for agricultural settings in central Belgium ($S = 0.02^* A_d^{-0.40}$) under a higher precipitation regime. The spatial distribution of the *SB* point cloud and the values of the a and b coefficients were not sensitive to different upslope lengths (2, 3, and 5 m) defining S: coefficient a was 0.02, 0.0175, and 0.0158 and b was −0.360, −0.355, and −0.387 for upslope lengths of 2, 3, and 5 m (Figure S2), suggesting that both the topographic thresholds for gully formation and the physical characteristics described by these parameters in the system are robust to the upslope length.

Each dataset from the literature that we compared with our data on topographic thresholds (Figure 5) used different cartographic products to measure Ad and S (especially upslope lengths). Vandekerckhove et al. (1998) used an upslope length that range from 2 to 4 m, which is comparable with our upslope length of 2 m, and sensitivity analysis on our data suggests that the topographical thresholds plot and regression coefficients a and b are insensitive to upslope lengths between 2 and 5 m (Figure S2). We conclude that the range of techniques and upslope lengths used by others does not complicate the comparison of results among studies.

Specific soil loss

A total of 311 polygons representing ephemeral gullies within 14 watersheds were identified and mapped from the orthophoto in the *SB* area. The width measured on the orthophoto

ranged from 0.3 to 3.1 m, and depth measured in the field ranged from 0.1 to 0.8 m. *SSL* decreased with increasing A_d in *SB* across two orders of magnitude in A_d (0.04 to 4 ha). *SSL* in *SB* was approximately 2–5 times higher than the mean of the sites from Castillo and Gómez (2016), which included sites with precipitation ranging from 40 to 215 mm (Table S4).

Mini-jet test analysis

The critical shear stress values obtained from the jet erosion test ranged from 1.4 to 1.9 Pa (1.6 Pa average), and soil detachment coefficient varied from 324 to 879 cm^3/Ns, suggesting high erodibility or low soil resistance values, according to Hanson's (1990) soil classification diagram. This is consistent with the difference between regression lines reported in this analysis, compared with area-SSL line from Castillo and Gómez (2016), with both indicating high vulnerability to gully erosion.

Discussion

Gully mapping

The study of gullies in rapidly urbanizing regions is particularly challenging due to (a) the ephemeral nature of the gullies, which may be filled in by maintenance crews within hours or days of a storm event, precluding use of historical aerial photographs to map them; and (b) the difficulty in delineating the watershed area draining to a given gully due to the complex drainage networks that form in urban areas. Although existing *DEMs* can be used to delineate watershed boundaries, they may become outdated as topography changes or have insufficient spatial resolution to accurately identify flow paths and watershed boundaries in a rapidly urbanizing environment. Microtopographic features such as roads, curbs, and ditches can change flow paths and watershed boundaries, and their relative impact on hydrology can be bigger in small watersheds. Both challenges require rapid, high-resolution mapping due to regular management practices implemented on roads that have impacts on gully networks and their contributing areas. *UASs–SfM* imagery and technology were used to address both challenges in *SB*.

Gullies formed almost exclusively on roads, reflecting their role in routing flow and their vulnerability to incision. Most gullies in *SB* are discontinuous because they are usually filled after storms, and the farthest downstream sections have lower slope and are more compacted due to vehicle traffic on the roads, all of which discourage gully formation.

Adediji et al. (2013) reported urban gullies on roads and adjacent to discontinuous concrete channels in Nigeria; gullies in other urban settings were formed in specific sites where runoff is concentrated (Archibold et al., 2003; Imwangana et al., 2014). Roads are the major component of anthropogenic sediment generation in the study area, which has also been reported in other settings, including logged forest (Montgomery & Dietrich, 1988; Reid & Dunne, 1984) and tropical islands (Ramos-Scharrón & MacDonald, 2007).

The high spatial resolution of the SfM-based *DSM* and orthophoto used in this research provided measurements of sufficient accuracy compared with those derived from other techniques and field-based measurements, representing an effective alternative to ground-

based measurements, especially for urban areas where representing complex drainage patterns and microtopographic features is important to accurate mapping of flow paths and A_d.

Topographical Thresholds

The roads in *SB* showed exceptional vulnerability to gully formation compared with other studies in a range of climates (Figure 5). Topographic thresholds for gully formation observed in *SB* were similar to gullies observed in Belgium and Portugal (annual precipitation of approximately 700 mm, and silty soils), but low threshold values of S and A_d for gully initiation in *SB* indicate greater vulnerability to gully erosion for a given storm event size, compared with thresholds values reported in Colorado (Patton & Schumm, 1975), Portugal, and Belgium (Vandaele et al., 1996) as well as California and Oregon (Montgomery & Dietrich, 1988).

Maugnard, Van Dyck, and Bielders (2014) suggested a potential bias on topographic thresholds using the lower envelope of the S–A_d relationship due to the high sensitivity to outlier values, though the *SB* point cloud is located generally lower than other point clouds from the literature (Figure 5). This vulnerability is explained in part by the fill materials used to repair gullies, which are typically unconsolidated sand and silt with low critical shear stress and high erodibility that increase gully erosion and sediment yield downstream. Roads also route and focus water flow along straight and steep flow paths, resulting in combinations of S and A_d that form gullies.

Comparing gully erosion studies that use different methods to determine gully formation thresholds is complicated, especially when case studies with different soils, geology, and climates are compared. Rainfall events with a high return period generate higher runoff and increase gully erosion for a given A_d (Vandaele, 1993), although ephemeral gully erosion will start only when a specific interaction of hydrologic, soil properties and management produce overland runoff that exceeds the critical soil shear stress to initiate and sustain gully erosion (Patton & Schumm, 1975; Vandaele et al., 1996). Rossi, Torri, and Santi (2015) noted potential biases in topographic thresholds studies, particularly overestimation of A_d in large watersheds (>30 ha), but this is not the case for the small watersheds of *SB*.

Urban development also impacts hydrological connectivity and runoff routing in ways that enhance potential for gully formation. Concrete lots, roofs, and parts of unpaved roads with low infiltration capacity generate runoff and route it to the roads, which increase storm water runoff and gully erosion.

Gully erosion rates

Decreasing sediment yield with increasing A_d was observed in *SB* (Figure 6), which is consistent with a sediment delivery ratio, the fraction of eroded sediment that is transported past the watershed outlet, of less than 1. Walling (1983) indicated that *sediment delivery ratio* tends to decrease with increased basin size, which has also been reported in other gully erosion studies (Castillo & Gómez, 2016; Poesen et al., 2003; Vandaele et al., 1996).

The highest *SSL* estimated in *SB* (7.4 mm/year) was generally higher than those reported in Castillo and Gómez (2016) for agricultural areas (Table S5 and Figure S1), Oygarden (2003) in Norway (3.7 mm/year), De Santisteban, Casali, and Lopez (2006) in Spain (5.9 mm/year), and Capra, Ferro, Porto, and Scicolone (2012) in Sicily (7.2 mm/year). Cases where gully erosion exceeded values observed in this study were reported by Martínez-Casasnovas et al., 2002in Spain (16.6 mm/year), which was associated with large precipitation events (215 mm over 135 min), and Tebebu et al. (2010) and Zegeye et al. (2016) in subhumid Ethiopia (up to 25 mm/year), which was associated with land use change and poor land management. Urban watershed characteristics such as vegetation removal, impervious surfaces, and hydrological connectivity due to roads can lead to increased gully erosion on unpaved roads. To our knowledge, this is the first attempt to quantify ephemeral gully erosion rates in urban environments at developing countries.

Urban gully erosion on unpaved roads from other studies (i.e., Adediji et al., 2013) was not normalized by time, complicating comparison with observed gully erosion rates in *SB*. Management practices in *SB*, especially road maintenance to fill gullies, represent an important contribution to total sediment production in *LLCW*.

Conclusions

Urbanization has important impacts on soil erosion rates. In the study area, gullies formed almost exclusively on unpaved roads, highlighting them as a major sediment source. Management practices, especially road maintenance that fill gullies with unconsolidated sediment, create an additional and continually replenished source of highly erodible sediment. Lower threshold values of S and A_d for gully incision were found in *SB* compared with agricultural environments, which is consistent with the high soil erodibility and low critical shear stress measured in the laboratory. Gully erosion rates in Tijuana were higher than almost all of those observed in agricultural watersheds described in the literature. Gully erosion may contribute significantly to the total sediment production, but other processes in the sediment budget need to be quantified for comparison.

The methodology described in this paper can be used in other watersheds to quantify gully erosion on unpaved roads. Our results suggest urgency in implementing management practices such as pavement or other stabilization of dirt roads to mitigate soil erosion. Future studies evaluating the effect of different soil types on gully erosion rates, as well as modeling the effect of road paving on runoff, soil erosion, and sediment loads, are crucial for proper management of sediment in our study area and potentially in urban areas in developing countries.

Supplementary Material

Refer to Web version on PubMed Central for supplementary material.

Acknowledgements

This study was funded by Consejo Nacional de Ciencia y Tecnología (CONACyT, México) and the U.S. Environmental Protection Agency (EPA; Interagency Agreement ID DW-12-92390601-0) in collaboration with the U.S. Department of Agriculture (USDA, Agreement 58-6408-4-015), San Diego State University (USA), University

of Córdoba (Spain), and the Centro de Investigación Científica y de Educación Superior de Ensenada (CICESE, México). Special thanks to Alejandro Hinojosa, Sergio Arregui, Belinda Sandoval, and Fernando Jauregui for their valuable help on data collection and processing. Alvaro Gomez-Gutierrez and two other reviewers provided valuable feedback on the manuscript. We thank Fran Rauschenberg, for review and technical editing.

References

Adediji A, Jeje LK, Ibitoye MO. 2013 Urban development and informal drainage patterns: Gully dynamics in Southwestern Nigeria. Applied Geography 40: 90–102. DOI: 10.1016/j.apgeog.2013.01.012

Al-Madhhachi AST, Hanson GJ, Fox GA, Tyagi AK, Bulut R. 2013 Measuring soil erodibility using a laboratory "mini" jet. Transactions of the ASABE 56(3): 901–910.

Archibold OW, Levesque LMJ, de Boer DH, Aitken AE, Delanoy L. 2003 Gully retreat in a semi-urban catchment in Saskatoon, Saskatchewan. Applied Geography 23: 261–279. DOI: 10.1016/j.apgeog.2003.08.005

Biggs TW, Atkinson E, Powell R, Ojeda L. 2010 Land cover following rapid urbanization on the US-Mexico border: Implications for conceptual models of urban watershed processes. Landscape and Urban Planning 96: 78–87. DOI:10.1016/j.landurbplan.2010.02.005

Capra A, Ferro V, Porto P, Scicolone B. 2012 Quantifying interrill and ephemeral gully erosion in a small Sicilian basin. Z. Geomorphology 56: 9–25. DOI:10.1127/0372-8854/2012/S-00070

Castillo C, Pérez R, James MR, Quinton NJ, Taguas EV, Gómez A 2012 Comparing the accuracy of several field methods for measuring gully erosion. Soil Science Society of America Journal 76: 1319–1332.

Castillo C, James MR, Redel-Macías MD, Pérez R, Gómez JA. 2015 SF3M software: 3-D photo-reconstruction for non-expert users and its application to a gully network. SOIL 1: 583–594. DOI: 10.5194/soil-1-583-2015

Castillo C, Gómez A. 2016 A century of gully erosion research: Urgency, complexity and study approaches. Earth-Science Reviews 160: 300–319.

De Santisteban LM, Casali J, Lopez JJ. 2006 Assessing soil erosion rates in cultivated areas of Navarre (Spain). Earth Surface Processes and Landform 31: 487–506. DOI:10.1002/esp.1281

Di Stefano C, Ferro V, Palmeri V, Pampalone V. 2017 Measuring rill erosion using structure from motion: A plot experiment. Catena 153: 383–392.

Dietrich JT. 2016 Riverscape mapping with helicopter-based Structure-from-Motion photogrammetry. Geomorphology 252: 144–157. DOI: 10.1016/j.geomorph.2015.05.008

Fonstad M, Dietrich JT, Courville BC, Jensen JL, Carbonneau PE. 2013 Topographic structure from motion: a new development in photogrammetric measurement. Earth Surface Processes and Landform 38: 421–430.

Foster GR. 1986 "Understanding Ephemeral Gully Erosion," Soil Conservation, Assessing the National Resource Inventory, National Academy of Science Press 2: 90–125.

Gómez-Gutiérrez A, Schnabel S, Lavado-Contador F. 2009 Gully erosion, land use and topographical thresholds during the last 60 years in a small rangeland catchment in SW Spain. Land Degradation &. Development 20 (5): 535–550. DOI: 10.1002/ldr.931

Gómez-Gutiérrez A, Schnabel S, Berenguer-Sempere F, Lavado-Contador F, Rubio-Delgado J. 2014 Using 3D photo-reconstruction methods to estimate gully headcut erosion. Catena 120: 91–101.

Guerra AJT, Hoffman H. 2006 Urban gully erosion in Brazil. Geography 19 (3): 26–29.

Hanson GJ. 1990 Surface erodibility of earthen channels at high stresses part II – developing an in situ testing device. Transactions of the ASAE 33 (1): 132−137.

Imwangana FM, Dewitte O, Ntombi M, Moeyersons J. 2014 Topographic and road control of mega-gullies in Kinshasa (DR Congo). Geomorphology 217: 131–139.

James MR, Robson S. 2012 Straightforward reconstruction of 3D surfaces and topography with a camera: Accuracy and geosciences applications. Journal of Geophysical Research 117: 1–17.

James MR, Robson S. 2014 Mitigating systematic error in topographic models derived from UAV and ground-based image networks. Earth Surface Processes and Landform 39: 1413–1420.

James MR, Robson S, d'Oleire-Oltmanns S, Niethammer U. 2017 Optimising UAV topographic surveys processed with structure-from-motion: Ground control quality, quantity and bundle adjustment. Geomorphology 280: 51–66.

Javernick L, Brasington J, Caruso B. 2014 Modeling the topography of shallow braided rivers using Structure-from-Motion photogrammetry. Geomorphology, 213, 166–182. DOI: 10.1016/j.geomorph.2014.01.006

Kakembo V, Xanga VW, Rowntree K. 2009 Topographic threshold in gully development on the hillslopes of communal areas in Ngqushwa local municipality, Eastern Cape, South Africa. Geomorphology 110: 188–194.

Martínez-Casasnovas JA, Ramos MC, Ribes-Dasi M. 2002 Soil erosion caused by extreme rainfall events: mapping and quantification in agricultural plots from very detailed digital elevation models. Geoderma 105: 125–140. DOI:10.1016/S0016-7061(01)00096-9.

Maugnard A, Van Dyck S, Bielders CL. 2014 Assessing the regional and temporal variability of the topographic threshold for ephemeral gully initiation using quantile regression in Wallonia (Belgium). Geomorphology 206: 165–177.

Micheletti N, Chandler JH, Lane SN. 2014 Investigating the geomorphological potential of freely available and accessible structure-from-motion photogrammetry using a smartphone. Earth Surface Processes and Landform 40: 473–486. DOI: 10.1002/esp.3648.

Momm HG, Bingner RL, Wells RR, Wilcox D. 2012 AGNPS GIS-based tool for watershed-scale identification and mapping of cropland potential ephemeral gullies. Applied engineering in agriculture 28 (1): 1–13. DOI: 10.13031/2013.41282

Montgomery DR, Dietrich WE. 1988 Where do channels begin? Nature 336: 232–234.

Montgomery DR, Dietrich WE. 1992 Channel initiation and the problem of landscape scale. Science 255: 826–830. [PubMed: 17756428]

Montgomery DR, Dietrich WE. 1994 Landscape dissection and drainage area-slope thresholds — Chapter 11 In: Kirkby MJ. (Ed.), Process Models and Theoretical Geomorphology. John Wiley & Sons Ltd, pp. 221–246.

Nachtergaele J, Poesen J. 1999 Assessment of soil losses by ephemeral gully erosion using high-altitude (stereo) aerial photographs. Earth Surface Processes and Landform 24: 693–706.

Nadal-Romero E, Revuelto J, Errea P, López-Moreno JI., 2015 The application of terrestrial laser scanner and SfM photogrammetry in measuring erosion and deposition processes in two opposite slopes in a humid badlands area (central Spanish Pyrenees). SOIL 1: 561–573.

Oygarden L 2003 Rill and gully development during an extreme winter runoff event in Norway. Catena 50: 217–242. DOI:10.1016/S0341-8162(02)00138-8.

Parkner T, Page MJ, Marutami T, Trustrum NA. 2006 Development and controlling factors of gullies and gully complexes. East coast, New Zealand. Earth Surface Processes and Landforms 31: 187–199.

Patton PC, Schumm SA. 1975 Gully Erosion, Northwestern Colorado: a threshold phenomenon. Geology 3: 88–90.

Poesen J, Govers G. 1990 Gully erosion in the loam belt of Belgium In: Boardman J, Foster IDL, Dearing J. (Eds.), Soil Erosion on Agricultural Land. Wiley, Chicester, pp. 513–530.

Poesen J, Nachtergaele J, Verstraeten G, Valentin C. 2003 Gully erosion and environmental change: importance and research needs. Catena 50: 91–133. DOI: 10.1016/S0341-8162(02)00143-1

Poesen JWA, Torri D, Vanwalleghem T. 2011 Gully erosion: procedures to adopt when modelling soil erosion in landscapes affected by gullying. Chapter 19 In: Morgan RPC, Nearing MA. (Eds.), Handboook of Erosion Modelling. Wiley-Blackwell ISBN: 978-1-4051-9010-7, pp. 360–386.

Ramos-Scharrón CE, MacDonald LH. 2007 Runoff and suspended sediment yields from an unpaved road segment, St. John, US Virgin Islands. Hydrological Processes 21: 35–50.

Reid LM, Dunne T. 1984 Sediment production from forest road surfaces. Water Resources Research 20 (11): 1753–1761.

Ries JB, Marzolff I. 2003 Monitoring of gully erosion in the Central Ebro Basin by largescale aerial photography taken from a remotely controlled blimp. Catena 50: 309–328. DOI: 10.1016/S0341-8162(02)00133-9.

Rossi M, Torri D, Santi E. 2015 Bias in topographic thresholds for gully heads. Natural Hazards 79: S51–S69. DOI: 10.1007/s11069-015-1701-2.

Tebebu TY, Abiy AZ, Zegeye AD, Dahlke HE, Easton ZM, Tilahun SA, Collick AS, Kidnau S, Dadgari F, Steenhuis TS. 2010 Surface and subsurface flow effect on permanent gully formation and upland erosion near Lake Tana in the northern highlands of Ethiopia. Hydrology and Earth System Sciences 14(11): 2207–2217. DOI:10.5194/hess-14-2207-2010.

Thorne CR, Zevenbergen LW, Grissinger EH, Murphey JB. 1986 Ephemeral gullies as sources of sediment. Proc. Fourth Federal Interagency Sedimentation Conf., Las Vegas, Nevada, 1, 3152–3.161.

Torri D, Sfalanga M, Chisci G. 1987 Threshold conditions for incipient filling. In: Bryan RB (Editor), Rill Erosion: Processes and Significance. Catena 8: 97–105.

Torri D, Poesen J. 2014 A review of topographic threshold conditions for gully head development in different environments. Earth-Science Reviews 130: 73–85. DOI: 10.1016/j.earscirev.2013.12.006.

Turner D, Lucieer A, Watson C. 2012 An automated technique for generating georectified mosaics from ultra-high resolution unmanned aerial vehicle (UAV) imagery, based on structure from motion (SfM) point clouds. Remote Sensing 4: 1392–1410.

Vandaele K 1993 Assessment of factors affecting ephemeral gully erosion in cultivated catchments of the Belgian Loam Belt In: Wicherek S (Editor), Farm Land Erosion in Temperate Plains Environment and Hills. Elsevier, Amsterdam, pp. 125–136.

Vandaele K, Poesen J, Govers G, van Wesemael B. 1996 Geomorphic threshold conditions for ephemeral gully incision. Geomorphology 16: 161–173.

Vanwalleghem T, Poesen J, Nachtergaele J, Verstraeten G. 2005 Characteristics, controlling factors and importance of deep gullies under cropland on loess-derived soils. Geomorphology 69: 76–91. DOI: 10.1016/j.geomorph.2004.12.003.

Walling D 1983 The Sediment Delivery Problem. Journal of Hydrology 65: 209–237. DOI: 10.1016/0022-1694(83)90217-2

Weis DA, Callaway JC, Gersberg RM. 2001 Vertical accretion rates and heavy metal chronologies in wetland sediments of the Tijuana Estuary. Estuaries 24: 840–850.

Westoby MJ, Brasington J, Glasser NF, Hambrey MJ, Reynolds JM. 2012 ‘Structure-from-Motion’ photogrammetry: A low-cost, effective tool for geoscience applications. Geomorphology 179: 300–314.

Wolman MG. 1967 A cycle of sedimentation and erosion in urban river channels. Geografiska Annaler A, 49: 385–395.

Zegeye AD, Langendoen EJ, Stoof CR, Tilahun SA, Dagnew DC, Zimale FA, Guzman CD, Yitaferu B, Steenhuis TS. 2016 Morphological dynamics of gully systems in the subhumid Ethiopian Highlands: The Debre Mawi watershed. SOIL 2(3): 443–458. DOI:10.5194/soil-2-443-2016.

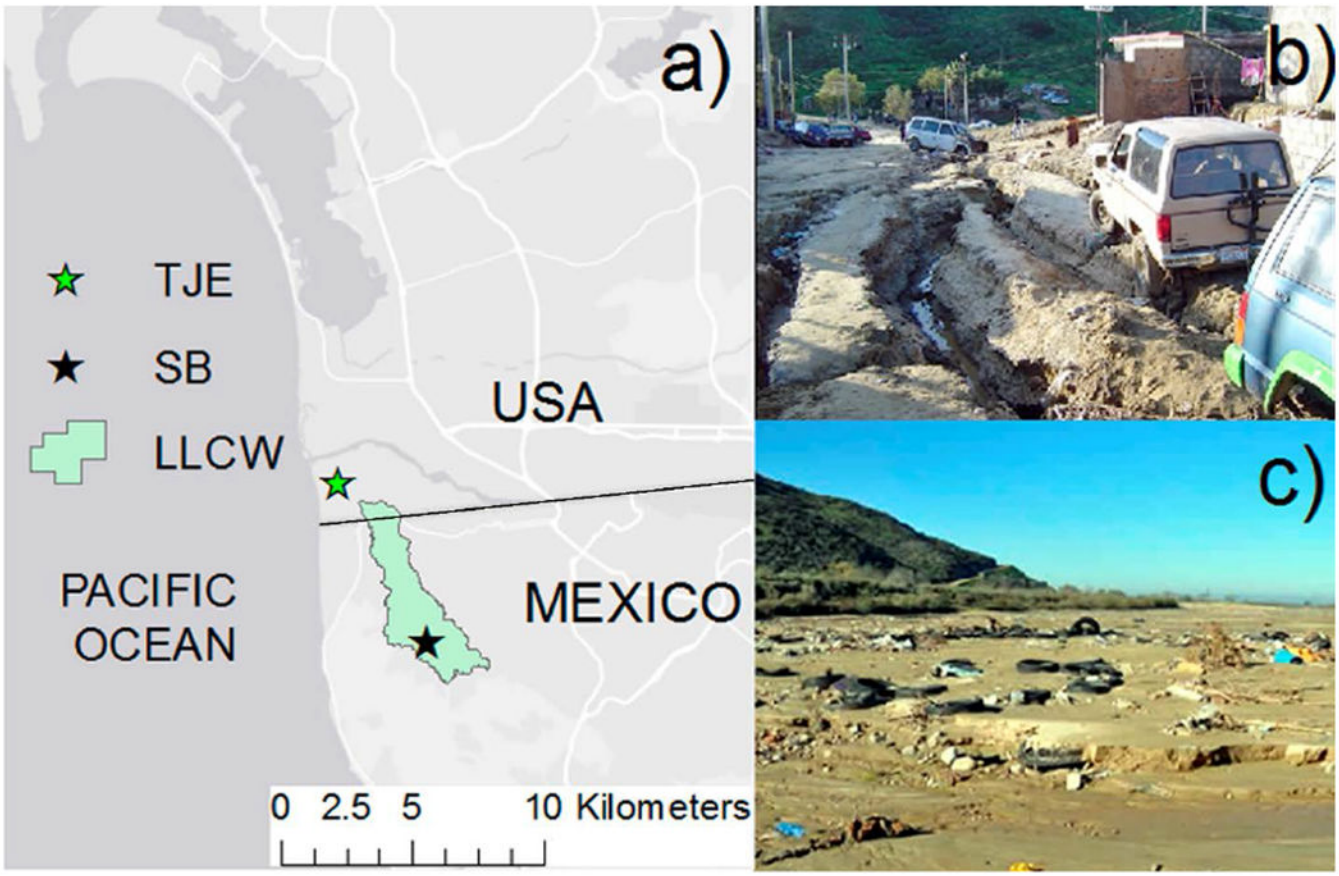

Figure 1.

a) Geographic location of Los Laureles Canyon Watershed (LLCW) and San Bernardo (SB), b) one example of land degradation caused by gully erosion in Tijuana, Mexico, c) excessive sedimentation in the Tijuana Estuarine Reserve (TJE), USA.

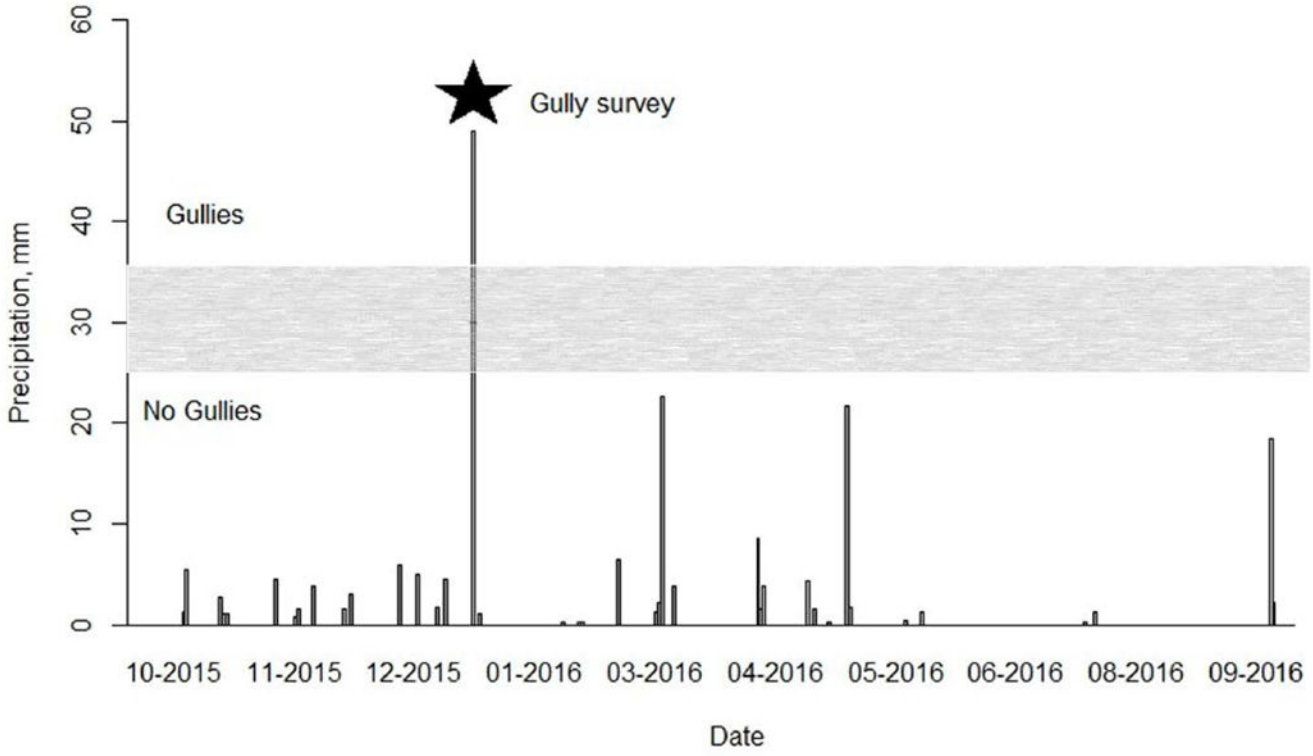

Figure 2.
Daily rainfall time series for the 2016 water year. The gray box represents the rainfall threshold (~25–35 mm) typically needed for gully formation in the study area.

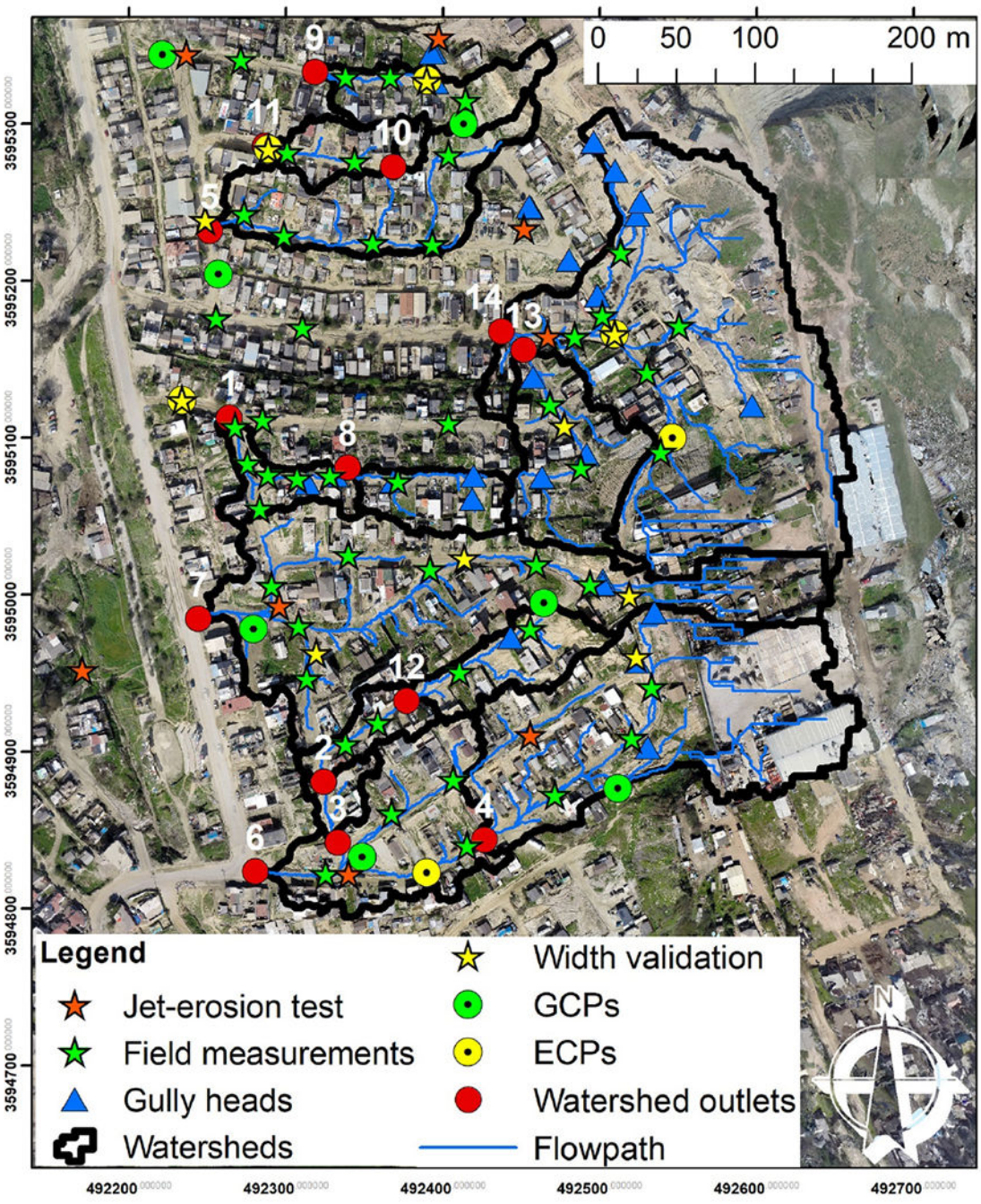

Figure 3.

Structure from motion-derived orthophoto and location of the study watersheds, ground control points (GCPs), error control points (ECPs), gully heads, and sampling locations

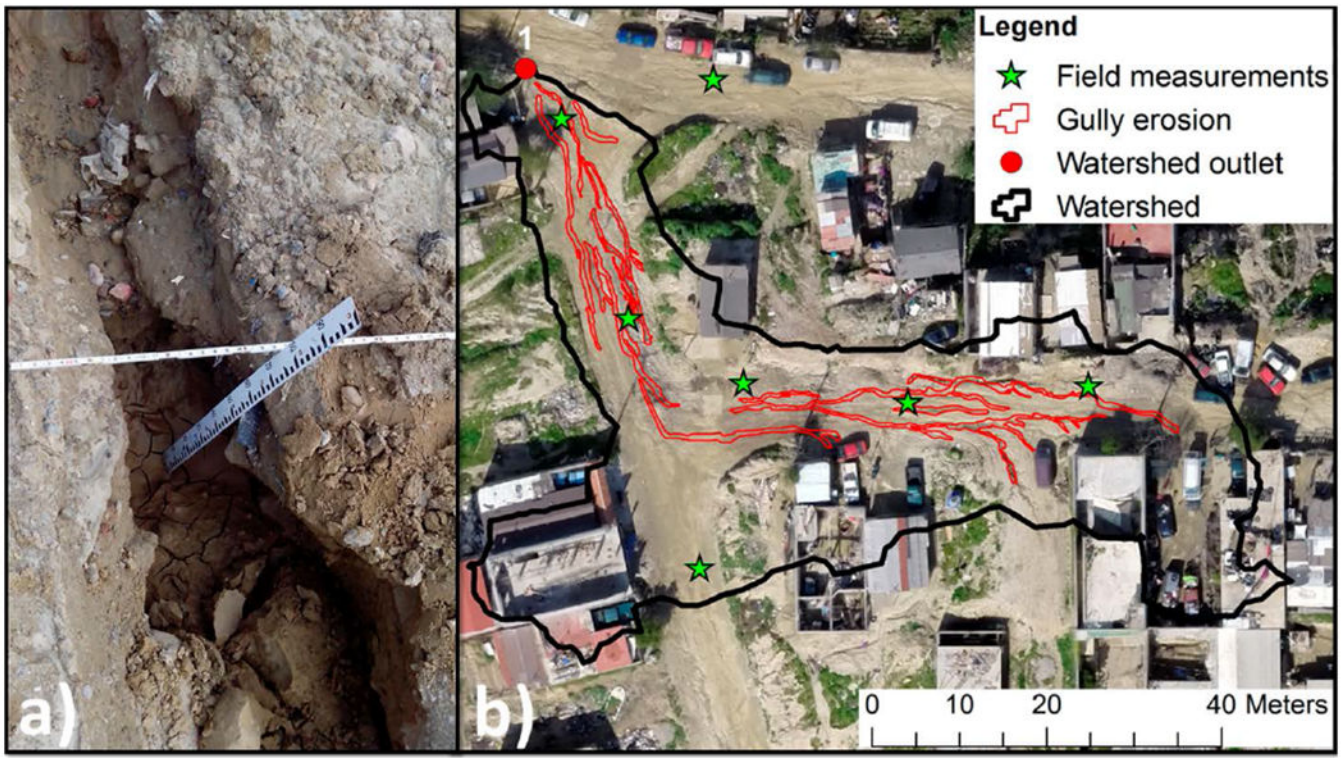

Figure 4.
Example of field measurements for watershed 1 (a) and measurement locations, digitized gullies, watershed boundary and outlet used to estimate specific soil loss (b).

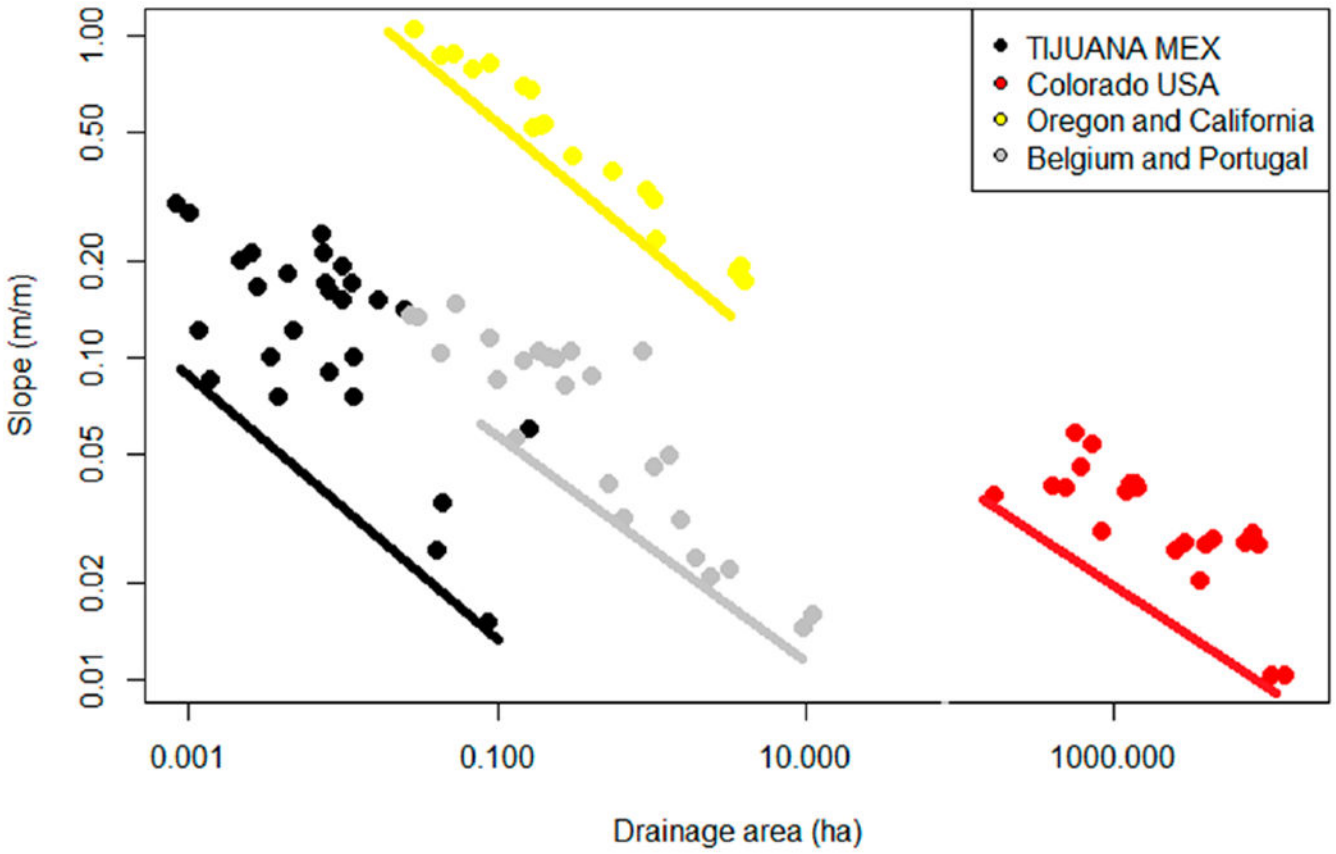

Figure 5.

Topographic thresholds (S and A_d) for the mapped headcuts in SB and from selected papers from literature; Colorado (Patton & Schummm, 1975); Oregon and California (Montgomery & Dietrich, 1988); Belgium and Portugal (Vandaele et al., 1995). The line fitted through the lower most points represents the critical conditions for gully initiation.

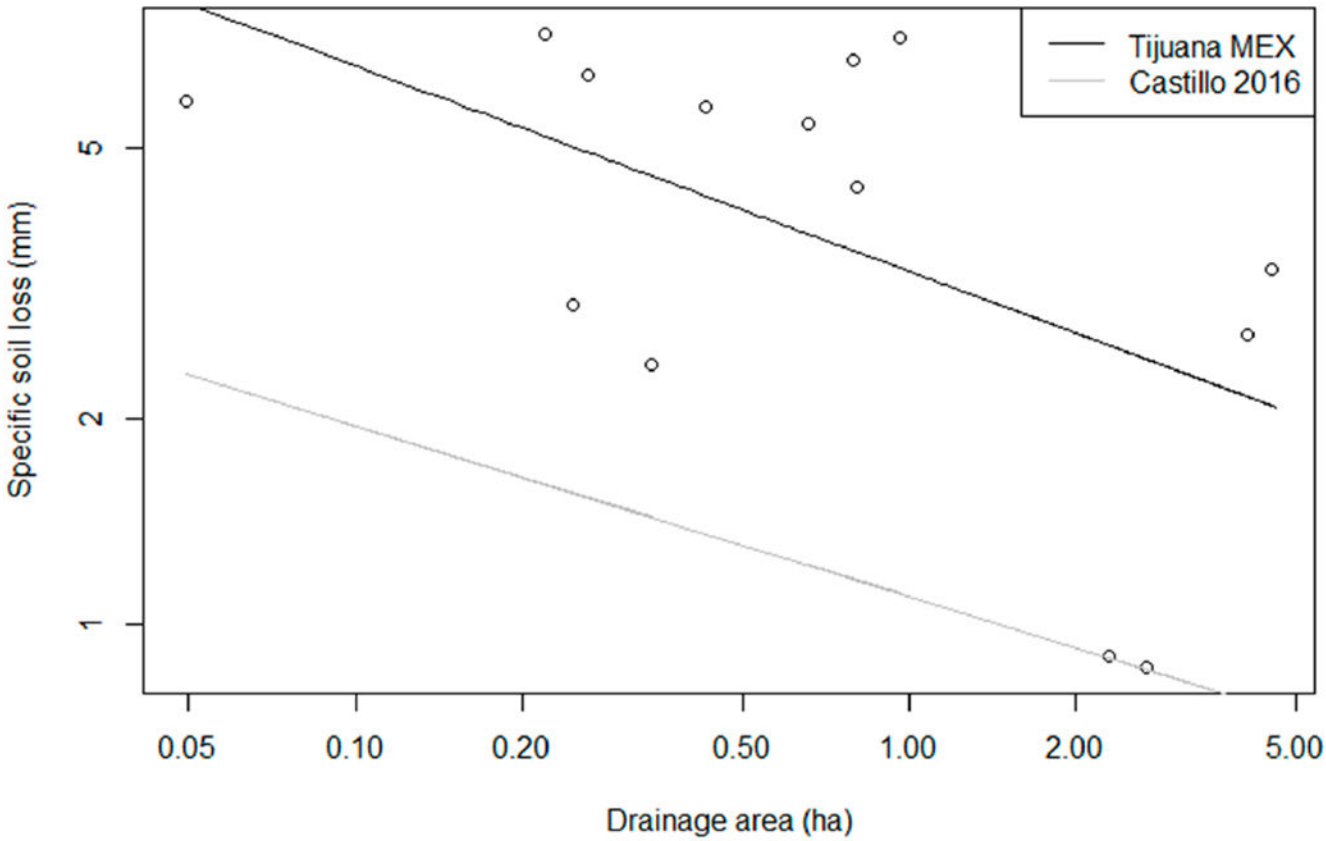

Figure 6.

Relationship between watershed size and *SSL* (Specific Soil Loss, the average depth of soil loss in the watershed) from gully erosion in *SB*, Tijuana, Mexico (circle points and black line). The gray line represent the average relationship reported by Castillo and Gomez (2016) for ephemeral gullies.